19th Symposium IMEKO TC 4 Symposium and 17th IWADC Workshop
Advances in Instrumentation and Sensors Interoperability
July 18-19, 2013, Barcelona, Spain

Geometric Feature Extraction for Precise Measurements in Intramedullary Nail images

Angelos Skembris[1], Elias Koukoutsis[1], Constantin Papaodysseus[1], Eleftherios Kayafas[1]

[1] National Technical University of Athens, 9 Iroon Polytexneiou, 15780, Zografou Athens, tel: 00302107722544, email: kayafas@cs.ntua.gr

Abstract- Closed Intramedullary Nailing (CIN) is a surgical procedure which requires that the surgeon accurately locates the optimal drilling position for inserting locking screws to stabilize and lock into position a nail inserted into the patient's bone. This procedure is difficult and is usually accomplished via X-ray fluoroscopic imaging, which results in large radiation exposure for both the patient and the surgical team. In this paper we present a method for making precise measurements of the nail geometric characteristics depicted in X-ray images in order to assist the surgeon during the determination of the nail body's position, assessment of any possible deformation during the insertion process, and the position and orientation of the nail holes' axes. This is achieved by firstly segmenting nail image to extract the area of the nail. Then, the nail body's shape is measured with the use of a deformable polygon that approximates the shape of the nail. The projections of the nail holes are then approximated with piecewise ellipses with the use of the Nelder-Mead minimization algorithm. Preliminary results show that using this method, we can achieve precise measurements of the nail body and hole projections in the X-ray image. These measurements can be used to construct a 3D model of the nail relative to the bone, which can in turn be used for the determination of the optimal drilling angle.

I. Introduction

In orthopaedic surgery, one of the most common methods of reducing fractures of long bones such as the femur and the tibia is Closed Intramedullary Nailing (CIN). During this surgical procedure, the surgeon first resets and realigns the bone and then makes an incision near one end of the broken bone. The procedure then calls for the drilling of a hole in the intramedullary canal of the bone so as to remove the bone marrow contained within the bone. This is performed in order to insert an intramedullary nail in the bone that will help stabilise the bone fragments during the healing process. In order to ensure that the fragments of the bone remain in place and aligned while the integrity of the fractured bone is restored through the natural healing process, the nail needs to be locked in position with respect to the bone fragments. This is achieved through the insertion of lateral screws in the proximal and the distal part of the nail. These screws ensure that the position of the nail remains locked relative to the realigned bone fragments [1].

This process of locking the nail into position often presents a challenge to the orthopaedic surgeon. The difficulties arise because during the insertion process, the nail may be deformed or rotated in order to conform to the shape of the bone canal. Due to this deformation, it is often difficult for the surgeon to establish the position and the axis of the holes that will receive the locking screws. The process of finding the exact position and direction of entry for the insertion of the screws often requires a large amount of anterior/posterior and lateral X-ray views, which results in the patient receiving large doses of radiation and a prolonged procedure duration, with a correspondingly increased risk of infection. [2-4]. Therefore, a system which provides an accurate depiction of the position and orientation of the locking holes to the surgeon, and in particular using only a few (or, ideally, one) X-ray images, would greatly improve this process resulting in fewer risks for the patient, less time spent in surgery and reduced cost.

Ideally, such a system would provide a comprehensive 3D view of the bone with the intramedullary nail inserted in it in order to provide the surgeon with a complete and accurate picture of the shape of the nail and the position and orientation of the holes relative to the bone. In this paper we present the first part of such a system, which deals with the extraction of geometric shape information from the shadow of the nail and its holes, as obtained from X-ray images of the nail by itself. In particular, we will present image processing and pattern recognition techniques for the accurate measurement of the nail characteristics (image preprocessing, segmentation, shape determination and geometric measurements). These measurements will then be used in conjunction with projection modelling to construct a 3D model of the nail and bone to establish the exact shape of the nail along with the position and orientation of the locking holes. These latter parts of the system will be presented in future reports.

ISBN-10: 84-616-5438-2 | ISBN-13: 978-84-616-5438-3

II. Related Work

The difficulties presented by the application of the CIN surgical technique have led to the development of different type of methodologies in order to assist the surgeons during the difficult part of locking the nail onto the bone. In general, these methodologies can be broadly classified into two categories: those that involve using a computer, and those that do not involve the use of computers.

Techniques that do not involve the use of computers make use of other tools that aid the surgeon during the procedure. The most common such technique is the freehand technique using an image intensifier, where the intensifier is aligned with the nail holes successively until the projection of the holes in the intensifier becomes a perfect circle [5]. Variations of this technique involve the use of mechanical targeting devices which are mounted onto the image intensifier and provide better guidance for the drill [6], or targeting devices mounted on the nail itself or the surgical table [7-8]

Computer assisted techniques range from x-ray modelling [9], pose detection [10-12], to complete robotic systems [13-14]. However, robotic systems are considered very expensive to implement and require sophisticated hardware and expert operators, while most pose detection methods are inflexible as to the shape deformation that the nail is subjected to during insertion, due to their use of the Hough transform for the nail body detection

In this paper, we present a method for accurate extraction of the nail and hole projection geometric characteristics that is insensitive to any such deformation, as it makes no assumptions concerning the shape of the nail projection other than the assumption that the projection is polygonal. The geometric characteristics extracted will be later used in the construction of a 3D model of the nail and bone in order to provide the surgeon with an accurate depiction of the position of the nail and the optimal drilling angle.

III. Methods

The methodology proposed here consists of the following steps: (a) Image Pre-processing, (b) Nail and hole area segmentation, (c) Extraction of geometric characteristics of the nail projection shape, and (d) Extraction of the geometric characteristics of the hole projection shape. In order to establish the validity of the approach, we examine here the results obtained by applying the methodology on X-ray images of the nail by itself. The results of applying the methodology on radiology images of actual nails inserted into bones will be presented in future reports.

A. Materials

The images we had at our disposal were of two types: (a) X-ray images of the nail that had been printed either on X-ray film or on paper and then scanned using a commercial scanner in two resolutions (150 and 300 DPI) and (b) digital X-ray images obtained directly from imaging devices capable of producing the end image in digital form. The images obtained were of the nail in several orientation, rotation and depression angles in order to test the performance of the algorithm in various conditions. The images were then cropped in order to separate the main body of the nail from the rest of the image (Figure 1(a)).

B. Image Pre-processing

In order to enhance the quality and contrast of the images, several preprocessing steps were taken. First, all the images were converted to grayscale (Figure 1(a)), and then a median filter with a 3x3 mask was applied in order to reduce the amount of noise present in the background and to preserve the edges. Subsequently, the histogram of the image was stretched so as to increase the contrast of the images and make edge detection and image segmentation easier.

ISBN-10: 84-616-5438-2 | ISBN-13: 978-84-616-5438-3

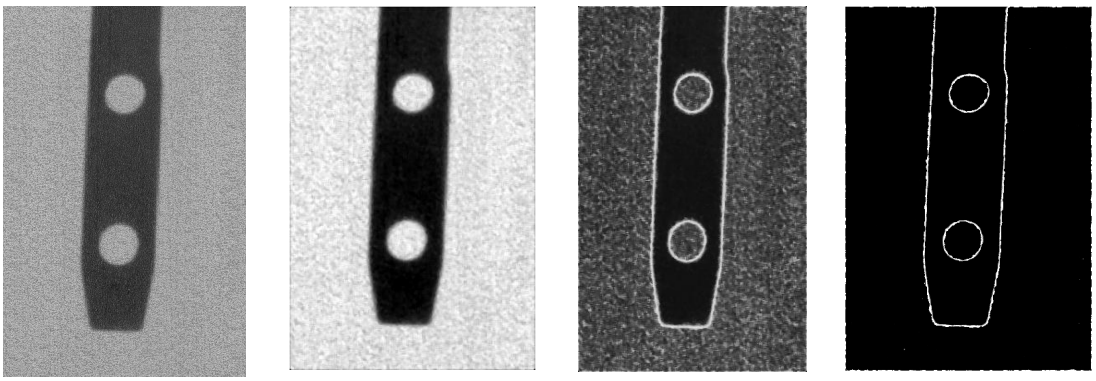

(a) (b) (c) (d)

Figure 1. Stages of nail image pre-processing and edge detection.

C. Image Segmentation

In order to obtain accurate geometric information, we require that the segmented area of the nail is connected. To achieve this, we used a combination of segmentation techniques including thresholding, edge detection and region growing. First, we select a point on the body of the nail which has a sufficiently low gray value on the contrast-enhanced image. In our case this was performed manually for greater accuracy, although it is easy to automate the process. Then, we construct a false colour image map of the differences of the levels of gray of the image pixels from the starting point and code this map using 64 distinct values in order to reduce the number of values to be examined. Using suitable colour coding, the false colour map can be adjusted so that pixels in the image having a large gray difference from the starting pixel yield an intermediate gray value when converted back to grayscale, whereas pixels with an intermediate difference yield a higher level of gray when converted back to grayscale (Figure 1(c)). Then, applying a threshold to the resulting image will give us a good estimate of the edges of the nail body along with the edges of the holes (Figure 1(d)).
By closing resulting image, we ensure that there are no gaps in the outline of the nail's body or the holes. Then, we perform region growing from the starting point using the edges of the nail body and the holes as boundaries of the region of interest. In this manner, we can extract the precise pixel locations of the nail's main body without including the projection shadows of the holes.

D. Geometric characteristic extraction of the nail's body.

Once we have located the pixels of the nail's body from our original image, we can now proceed with extracting geometrical information from this region. This first step for this is to enumerate the outline of the nail's body. This process is completed automatically through the use of an algorithm developed for this purpose, and during the enumeration we remove any right angles, pixel "tentacles" (i.e. chains of single pixels that stem from the body of the region) and other artefacts that might adversely affect our calculations.
We then proceed to determine the turning points, or angles, of the outline of the nail. To achieve this, for every pixel belonging to the enumerated outline of the nail we calculate the optimal in the LS sense straight line segments that approximate the previous and next 30 pixels on either side of the current pixel. Then, we calculate the value of the angle between the two straight line segments for every pixel of the outline of the nail's body. The local maxima of the angle values constitute the turning points, i.e. the angles of the outline. After filtering the angle value "signal" to eliminate the noise present (Figure 2(a), we use the indices of the angle value vector where the local maxima occur to establish the locations of the nail outline's turning points (Figure 2(b)). In order to avoid pseudo-maxima that occur due the noise introduced in the process by the constant shifting of the examined pixel and the re-calculation of the LS straight line segments, we set a threshold of 8 degrees as the minimum angle a turning point can have.
Due to the way the angle value is calculated, there may be cases where the maximum value of the angle does not occur at the correct pixel of the nail's outline, and it occurs a few pixels on either side of the optimal position. This can be seen as an example in Figure 2(b), where the position of turning points 6 and 7 (counting clockwise, with 1 being the top left turning point) are clearly not the optimal positions. In order to get more precise measurements, we need to refine and optimize the positions of the turning points so that our polygonal shape

ISBN-10: 84-616-5438-2 | ISBN-13: 978-84-616-5438-3

approximation fits the outline of the nail's body with greater precision. For this reason we developed the following iterative algorithm:

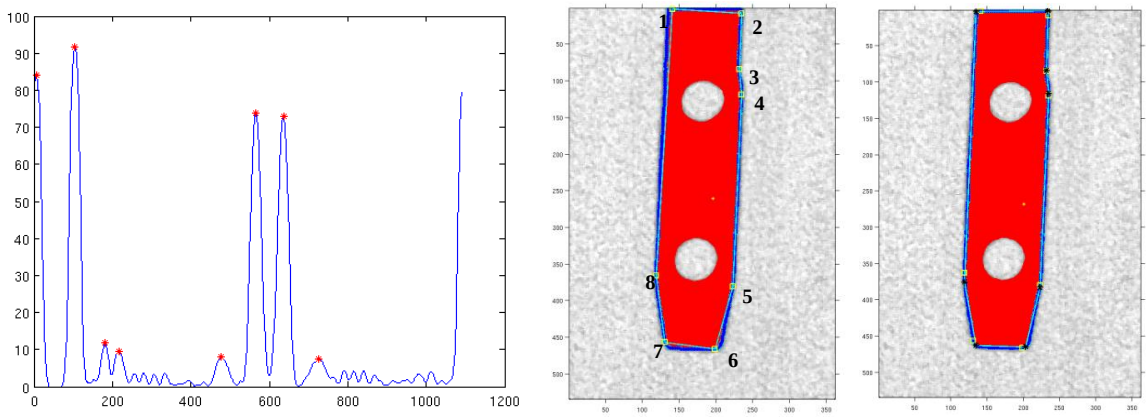

(a) (b) (c)

Figure 2. (a) Plot of angle values. (b) Initial estimate of turning points. (c) Improved estimate of turning points

First, we divide the outline of the nail's body into segments, each of which has as a starting and ending point two consecutive turning points, as they were initially estimated using the procedure described previously. Then, we calculate the sum of the distances of the outline pixels of each such segment from the corresponding points of the LS straight line segments approximating these segments, and sum all those error values in order to obtain a total approximation error for these particular turning point locations. In order to reduce this total error value, for each turning point we shift the location of the turning point by a few indices (plus or minus) on the outline coordinates vector, which results in a shifting of the position of the turning point along the outline. For each new position, we calculate the total error again, and if the new value of the total error is lower than the previous value, the new position of the turning point is considered to be a better estimate of the turning point coordinates than the old one. For every instance that we obtain a lower value of the total error, we repeat this process from the beginning, since an improved location estimate for one of the turning points may lead to a re-evaluation and better fit for the adjacent turning points as well.
Using this process, we obtain the optimal turning point locations (Figure 2(c), with the improved estimates of the turning points shown in black), and can thus approximate the outline of the nail using a deformable polygonal shape, the geometric characteristics of which are now very easy to establish and compare to known values. This procedure is robust, has low computational demands and can be used to extract the geometric characteristics of any polygonal shape. Also, the precise nature of the measurements means that the user of the system can easily establish whether the nail body has been deformed during the insertion process.

E. Geometric characteristic extraction of the hole projections.

We now proceed to extract the geometric characteristics of the hole projections. First we proceed to establish the number of holes in our image and enumerate their outline, as done previously. In order to do this, we first find the set of pixels of the region of interest that do not belong to the nail body outline and have at least one neighboring pixel that does not belong to the nail's body. These pixels obviously form the outlines of the holes' projections. We start at a random pixel and then proceed to find a neighboring pixel that also belongs to the hole outline pixel set. This process is repeated until there are no more neighboring pixels available, i.e. the outline of the particular hole has come full circle and is now closed. If there are any remaining pixels in the hole outline pixel sets, then there is more than one hole in our image (the number of holes is not always known, as different types of nails may have a different number of holes), and the hole count is increased by one. We then repeat the process starting at a random pixel of the remaining pixels in the set, each time increasing the hole count when a hole outline becomes closed. In this manner, we can determine the number of holes and their consecutively enumerated outline pixels.
We then proceed to extract some geometric characteristics of the hole projections. In this case we assumed that the holes in question are cylindrical and therefore their projections will be circular, elliptical or piece-wise elliptical in shape. This is not always the case, as different types of nails may have different shaped holes,

ISBN-10: 84-616-5438-2 | ISBN-13: 978-84-616-5438-3

however the procedure presented here can be used with any explicitly defined curve.
In order to extract the geometric characteristics of each hole, we first determine its outline's center of mass, and its axes of symmetry. The minor and major axes of symmetry were initially estimated as the lengths of straight line segments connecting the center of mass with the nearest and farthest pixel of the hole's outline, respectively. Also, the angle of rotation of the hole was initially estimated as the angle of the major axis with the horizontal. Using these initial values as parameter estimates, we then applied the Nelder-Mead minimization algorithm in order to minimize the error between the hole outline and an ideal ellipse with variable parameters, and consequently obtain an estimate of the parameters of the ideal ellipse that best approximates the hole outline. In our case, the error measure to be minimized was the average of the distances of the ideal ellipse points from the corresponding hole outline pixels along the direction of the radius passing from the origin, after the hole outline had been rotated and translated so that its center was the origin and its major axis was parallel to the x-axis.
We applied three variations of this approach. For the first variation (Figure 3(a)), we assumed that the ideal ellipse center was identical to center of mass of the hole outline. This approach yielded sub-pixel average errors for images where the nail had been depicted with little or no rotation about its longitudinal axis. These results were slightly improved with the application of our second variation, where the center of the ideal ellipse was also allowed to vary. In this case the initial estimate of the center of the ideal ellipse was the center of mass of the hole outline. This approach yielded slightly better results (Figure 3(b)), again for images where there was not much rotation of the nail.
When the rotation of the nail was such that the holes became only piecewise elliptical, both these approaches yielded larger values for the minimum error. In those cases, our third variation improved the results. For the third variation, the outline of the hole was divided into two approximately equal sections, with the estimate of the major axis providing the boundary points. Then, the two parts were individually approximated by ideal ellipse sections, with free centers and the additional error constraint that the difference between the length of the hole outline section and the length of the ideal ellipse section was added to the total error to be minimized. Using this approach, we obtained visually better fits for almost all cases (Figure 3(c)), although the error values were not directly comparable to the other two approaches due to the different error measure.

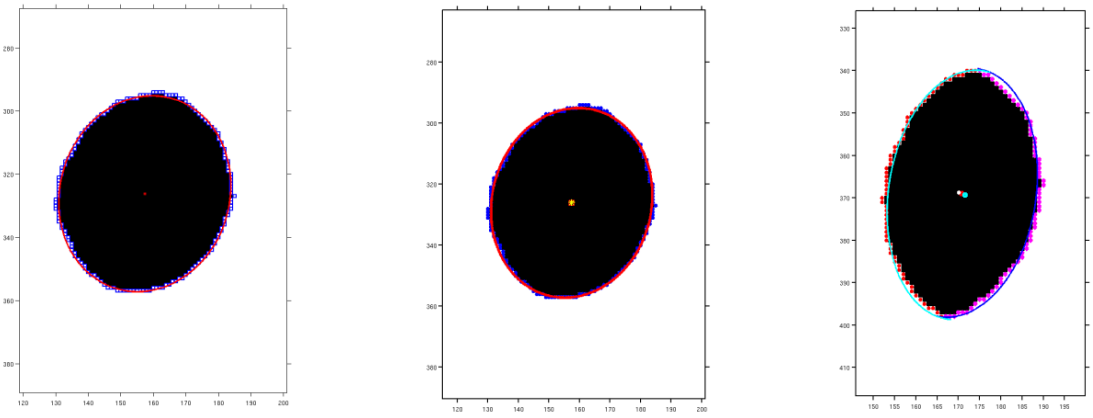

(a) (b) (c)

Figure 3. Approximation of the hole outline shape with (a) an ideal ellipse with the same center, (b) an ideal ellipse with free center (c) piecewise elliptical sections.

IV. Conclusions and further research

In this paper we have demonstrated methodologies for geometric feature extraction and precise measurements from X-ray images of intramedullary nails. These measurements can be used to establish whether the nail has suffered deformation during its insertion to the bone by the surgeon, as well as the angle of rotation of the nail's holes. This information can be used to determine the optimal drilling hole for the insertion of the locking screws that will lock the nail into position and stabilize it during the bone's healing process.

ISBN-10: 84-616-5438-2 | ISBN-13: 978-84-616-5438-3

The next steps in this project involve the application of the above methodology to actual images of intramedullary nails inserted in the bone before the insertion of the locking screws, so that the algorithms are adapted to account for the presence of the bone in the X-ray image. This will be followed by the construction of a 3D projection model for the nail, initially, and the bone. Using the measurements obtained by applying the methodologies presented above in conjunction with the projection model, we hope to construct a comprehensive 3D depiction of the bone with the nail inside it. Using this 3D projection, the next step is to determine the optimal drilling angle for the insertion of the locking screws. It is our expectation that once the system has been completed, using only a few X-ray images it will be able to aid the surgeon in performing the difficult procedure of drilling, thus reducing radiation exposure time for the surgeon and the patient, reducing the risk of erroneous drilling and shortening the duration and the cost of the procedure. We also expect that this system will be much cheaper to implement than other systems currently in use.

References

[1] R. J. Brumback, "The rationales of interlocking nailing of the femur, tibia, and humerus: an overview", *Clinical Orthopaedics and Related Research.*, vol. 324, pp. 292–320, 1996.
[2] Moreau JP, Ashmore JP. "Radiation exposure to the surgeon during Ender's nailing", *Canadian Journal of Surgery*, vol. 29, pp 82-28, 1986.
[3] Muzaffar TS, Imran Y, Iskandar MA, et al. "Radiation exposure to the surgeon during femoral interlocking nailing under fluoroscopic imaging.", *Medical Journal of Malaysia*, vol. 60(C), pp. 26-9, 2005
[4] S. Skjeldal and S. Backe, "Interlocking medullary nails—radiation doses in distal targeting," *Archives of Orthopaedic and Trauma Surgery*, vol. 106, pp. 179–181, 1987.
[5] Medoff RJ. "Insertion of the distal screws in interlocking nail fixation of femoral shaft fractures.", Technical note. *The Journal of Bone & Joint Surgery, American Edition*, vol. 68, pp. 1275—7, 1986.
[6] Kempf I, Leung KS. *Practice of Intermedullary Locked Nails. Scientific basis and Standard Techniques*. Springer Verlag, Berlin Heidelberg, 2002.
[7] Tyropoulos S, Garnavos C. "A new distal targeting device for closed interlocking nailing", *Injury*, vol.32, pp. 732-5, 2001.
[8] Y. Arlettaz, A. Akik , F. Chevalley , P.F. Leyvraz, "Targeting device for intramedullary nails: A new high-stable mechanical guide",.*Injury*, vol. 39, pp. 170—175, 2008.
[9] Z.G. Kamarianakis, I.G. Buliev, and N.E. Pallikarakis, "Identification and Localization of Intramedullary Nail Holes for Orthopedic Procedures Using Cone Beam Reconstruction and Simulation Techniques", *IFMBE Proceedings*, Vol. 25(4), pp 1182-1185, 2010,
[10] Zheng G, Zhang X, Haschtmann D, Gédet P, Langlotz F, Nolte LP. "Accurate and reliable pose recovery of distal locking holes in computer-assisted intra-medullary nailing of femoral shaft fractures: a preliminary study.", *Computer Aided Surgery*, vol. 12(3), 138-51, 2007.
[11] Zheng G, Zhang X, Haschtmann D, Gedet P, Dong X, Nolte LP. "A robust and accurate two-stage approach for automatic recovery of distal locking holes in computer-assisted intramedullary nailing of femoral shaft fractures", *IEEE Transactions on Medical Imaging*. Vol. 27(2), pp. 171-87, 2008 Feb;27(2):171-87.
[12] Neatpisarnvanit, C., Suthakorn, J. "Intramedullary Nail Distal Hole Axis Estimation using Blob Analysis and Hough Transform". *IEEE International Conference on Robotics, Automation and Manufacturing (RAM 2006)*, Bangkok, Thailand, June 7-9, 2006.
[13] Yao, J., Taylor, R. H., Goldberg, R. P., Kumar, R., Bzostek A., Van Vorhis, R., Kazanzides P., Gueziec A., "A C-Arm Fluoroscopy-Guided Progressive Cut Refinement Strategy Using a Surgical Robot", *Computer Aided Surgery*, vol. 5, pp. 373–390, 2000.
[14] Yaniv Z., Joskowicz, L. "Precise Robot-Assisted Guide Positioning for Distal Locking of Intramedullary Nails.", *IEEE Transactions on Medical Imaging*, vol. 24(5), pp. 624-35, 2005